Accurate Reduced Order Models for Coherent Synchronous Generators

Hancheng Min, and Enrique Mallada
Johns Hopkins University, Baltimore, MD, U.S.A.
Email: {hanchmin, mallada}@jhu.edu

Fernando Paganini
Universidad ORT Uruguay, Montevideo, Uruguay
Email: paganini@ort.edu.uy

arXiv:1909.12864v2 [eess.SY] 4 Oct 2019

***Abstract*—We introduce a novel framework to approximate the aggregate frequency dynamics of coherent synchronous generators. By leveraging recent results on dynamics concentration of tightly connected networks, we develop a hierarchy of reduced order models –based on frequency weighted balanced truncation– that accurately approximate the aggregate system response. Our results outperform existing aggregation techniques and can be shown to monotonically improve the approximation as the hierarchy order increases.**

***Index Terms*—model reduction, frequency response, coherence**

I. Introduction

Accurately modeling generator frequency response to power disturbances is essential for assessing frequency control performance in power grids. Techniques for deriving reduced order approximations of large-scale power networks based on *coherence* and *aggregation* have been investigated for decades [1]. Generally, a group of generators is considered coherent if their bus frequencies exhibit a similar response when subject to power disturbances. A widely used modeling technique is to subsequently aggregate the response of coherent generators into a single effective machine.

In past decades, various methods for identifying coherent group of generators have been introduced [2]–[7]. The Linear Simulation Method [8] groups generators whose maximum difference in time-domain response is less than some tolerance. Similarly, [3] develops a clustering algorithm based on the pairwise maximum difference in time-domain response, which is extended to the frequency-domain in [4]. The Weak Coupling Method [7] quantifies strength of coupling between two areas to iteratively determine the boundaries of coherent generator groups. The Two Time Scale Method [5], [6] computes the eigen basis matrix associated with the electromechanical modes in the linearized network: two generators with similar entries on the basis matrix with respect to low frequency oscillatory modes are considered coherent.

Once all generators are grouped by coherence, each group can be aggregated into a single effective machine. Previous work [9]–[14] has demonstrated that the best choice of inertial and damping coefficients for the effective generator is obtained by adding among all the corresponding generator parameters. However, in the presence of turbine dynamics, the proper choice of turbine time constants is challenging. Optimization-based approaches [10], [11] minimize an error function to choose the time constant of the effective generator. Other approaches use the average [12], or the weighted harmonic mean [13] of time constants of generators in the coherent group. However, these methods cannot in general achieve high accuracy in capturing the coherent frequency response.

In this paper, we leverage new results on characterizing coherence in tightly-connected networks [15] to introduce a general framework for aggregation of coherent generators. We show that for n coherent generators with transfer function $g_i(s),\ i = 1, \cdots, n$, the aggregate coherent dynamics are accurately approximated by $\hat{g}(s) = \left(\sum_{i=1}^{n} g_i^{-1}(s)\right)^{-1}$. Moreover, we show that $\hat{g}(s)$ is a natural characterization of the coherent dynamics in the sense that, as the algebraic connectivity of the network increases, the response of the coherent group is asymptotically $\hat{g}(s)$. In the case of heterogeneous turbine dynamics, the aggregate dynamics $\hat{g}(s)$ can be as high order as the network size n, then the aggregation of generators essentially asks for a low-order approximation of $\hat{g}(s)$. In order to obtain the accurate approximation of $\hat{g}(s)$, we propose a hierarchy of reduced order models, based on frequency weighted balanced truncation, which not only offers as reduced model a single effective generator, but also higher-order reduction model with significantly improved accuracy.

Our result shows that aggregation of coherent generators can be regarded as finding a low-order approximation of $\hat{g}(s)$. In the case of high-order $\hat{g}(s)$, the conventional approaches [10], [11], [13] are too restrictive, where the approximation model is given by a single effective generator with proper time constant and all other parameters chosen as their aggregate value. Our proposed models suggests two potential improvements by enforcing less constraints: 1) Increase the order of the approximation model, and in particular for 2nd order generator model, a 3rd order reduction model of $\hat{g}(s)$ is almost accurate; 2) Model reduction on closed-loop dynamics $\hat{g}(s)$ instead of on high-order turbine dynamics. Lastly, the aggregation techniques introduced in this paper apply to any linear model of generators, allowing us to obtain accurate aggregate higher order generator models.

The rest of the paper is organized as follows. In Section II, we provide the theoretical justification of the coherent dynamics $\hat{g}(s)$. In Section III, we propose reduced order models for $\hat{g}(s)$ by frequency weighted balanced truncation. We then show via numerical illustrations that the proposed models can achieve accurate approximation (Section IV). Lastly, we

This work was supported by US DoE EERE award de-ee0008006, NSF through grants CNS 1544771, EPCN 1711188, AMPS 1736448, and CAREER 1752362, Johns Hopkins University Discovery Award, and ANII-Uruguay, through grant FSE_1_2017_1_145060,

conclude this paper with more discussions on the implications of our current results.

II. Aggregate Dynamics of Coherent Synchronous Generators

Consider a group of n generators, indexed by $i = 1, \cdots, n$, dynamically coupled through an AC network. Assuming the network is in steady-state, the block diagram of linearized system around this operating point is shown in Fig.1.

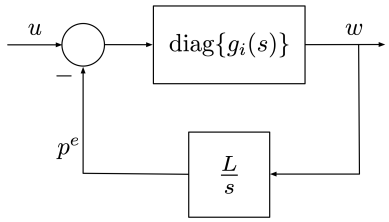

Fig. 1. Block Diagram of Linearized Power Networks

For generator i, the transfer function from net power deviation at its generator axis to its angular frequency deviation w_i, relative to their equilibrium values, is given by $g_i(s)$. The net power deviation at generator i, includes disturbance u_i reflecting variations in mechanical power or local load, minus the electrical power p_i^e drawn from the network.

The network power fluctuations p^e are given by a linearized (lossless) DC model of the power flow equation

$$p^e(s) = \frac{1}{s} L w(s)\,,$$

where we use the standard convention of 's' to refer to the Laplace domain and 't' for time domain. Here L is the Laplacian matrix of an undirected weighted graph, with its elements given by

$$L_{ij} = \left.\frac{\partial}{\partial \theta_j} \sum_{k=1}^{n} |V_i||V_k| b_{ik} \sin(\theta_i - \theta_k) \right|_{\theta=\theta_0},$$

where θ_0 are angles at steady state, $|V_i|$ is the voltage magnitude at bus i and b_{ij} is the line susceptance. Without loss of generality, we assume the steady state angular difference $\theta_{0i} - \theta_{0j}$ across each line is smaller than $\frac{\pi}{2}$. Moreover, because L is a symmetric real Laplacian, its eigenvalues are given by $0 = \lambda_1(L) \le \lambda_2(L) \le \cdots \le \lambda_n(L)$. Particularly, the *algebraic connectivity* $\lambda_2(L)$ is positive if the network is connected [16]. The overall linearized frequency dynamics of the generators is given by

$$w_i(s) = g_i(s)(u_i(s) - p_i^e(s)), \quad i = 1, \cdots, n \tag{1a}$$

$$p^e(s) = \frac{1}{s} L w(s)\,. \tag{1b}$$

In this section, we are interested in characterizing the dynamic response of coherent generators to system disturbances, which we term here *coherent dynamics*. With this aim, we seek conditions on the network (1) under which the entire set of generators behave coherently. The same approach can be used on subgroups of generators.

To motivate our results, we follow typical assumptions, e.g., equal frequency response $w_i(s) = \hat{w}(s)$ among coherent generators [9]–[11], to derive a closed form expression for the coherent dynamics; the basic theory that justifies this derivation is then provided in Section II-A. By assuming $w_i(s) = \hat{w}(s)$, it is possible to sum over all equations in (1a) to get

$$\left(\sum_{i=1}^{n} g_i^{-1}(s)\right) \hat{w}(s) = \sum_{i=1}^{n} u_i(s) - \sum_{i=1}^{n} p_i^e(s)\,. \tag{2}$$

Notice that the last term $\sum_{i=1}^{n} p_i^e(s) = \mathbb{1}^T \frac{L}{s} \mathbb{1} \hat{w}(s) = 0$ since $\mathbb{1} = [1, \cdots, 1]^T$ is an eigenvector of $\lambda_1(L) = 0$. Then the aggregate model for the coherent group is given by

$$\hat{w}(s) = \left(\sum_{i=1}^{n} g_i^{-1}(s)\right)^{-1} \sum_{i=1}^{n} u_i(s)\,. \tag{3}$$

From (3), the coherent group of generators is aggregated into a single effective machine with its transfer function given by

$$\hat{g}(s) = \left(\sum_{i=1}^{n} g_i^{-1}(s)\right)^{-1}. \tag{4}$$

While insightful and novel, equation (4) is not properly substantiated. In what follows we provide a principled justification for using (4) as our model for the coherent dynamics by leveraging recent results on coherence of tightly connected networks [15].

A. Coherence in Tightly Connected Networks

We now lay down the basic theory that justifies the use of (4) as an accurate descriptor of the dynamics of coherent generators. Our analysis, in particular, will highlight the role of the algebraic connectivity $\lambda_2(L)$ of the network as a direct indicator of how coherent a group of generators is.

For the network shown in Fig.1, the transfer matrix from the disturbance u to the frequency deviation w is given by

$$T(s) = \left(I_n + \mathrm{diag}\{g_i(s)\}\frac{L}{s}\right)^{-1} \mathrm{diag}\{g_i(s)\}\,, \tag{5}$$

where I_n is the $n \times n$ identity matrix. To justify the coherent response of generators, we show that the transfer matrix $T(s)$ converges, as algebraic connectivity $\lambda_2(L)$ increases, to one where all entries are given by $\hat{g}(s)$.

We make the following assumptions:

1) $T(s)$ is stable;
2) all $g_i(s)$ are minimum phase systems;
3) $\hat{g}(s)$ in (4) is stable.

For generators that satisfy these assumptions, we have the following result.

Theorem 1. *Given the assumptions above, the following holds for any $\eta_0 > 0$:*

$$\lim_{\lambda_2(L)\to+\infty} \sup_{\eta\in[-\eta_0,\eta_0]} \left\| T(j\eta) - \hat{g}(j\eta)\mathbb{1}\mathbb{1}^T \right\| = 0\,,$$

where $j = \sqrt{-1}$ and $\mathbb{1} \in \mathbb{R}^n$ is the vector of all ones.

The proof is shown in the appendix. The analysis relies on the fact that $T(s)$ is close to $\hat{g}(s)\mathbb{1}\mathbb{1}^T$ if the *effective algebraic connectivity* $\left|\frac{\lambda_2(L)}{s}\right|$ is large. For any frequency band $[-j\eta_0, j\eta_0]$ on the imaginary axis, the effective algebraic connectivity is lower bounded by $\frac{\lambda_2(L)}{\eta_0}$, hence one can make sure $T(s)$ is arbitrarily close to $\hat{g}(s)\mathbb{1}\mathbb{1}^T$ on this frequency band by increasing $\lambda_2(L)$.

The transfer matrix $\hat{g}(s)\mathbb{1}\mathbb{1}^T$ can be interpreted as follows. Given any arbitrary disturbance $u(s)$, the frequency response to such disturbance is given by

$$w(s) = \hat{g}(s)\mathbb{1}\mathbb{1}^T u(s) = \left(\hat{g}(s)\sum_{i=1}^{n} u_i(s)\right)\mathbb{1}. \tag{6}$$

In other words, every bus frequency reacts to the aggregate disturbance $\sum_i u_i(s)$ based on the response $\hat{g}(s)$. As a result, for any disturbance limited over band $[0, \eta_0]$, the response of the network $T(s)u(s)$ approximates the one of (6). Therefore generator networks with large algebraic connectivity should be considered a coherent group.

On the other hand, such coherence among generators is frequency-dependent: As we suggested above, the effective algebraic connectivity $\left|\frac{\lambda_2(L)}{s}\right|$ determines how close $T(s)$ is to $\hat{g}(s)\mathbb{1}\mathbb{1}^T$ at certain point. For any fixed $\lambda_2(L)$, there is a large enough cutoff frequency η_c such that $\left|\frac{\lambda_2(L)}{j\eta}\right|$ is sufficiently small for any $\eta \geq \eta_c$, which is to say, for certain coherent group of generators, the responses of generators are not coherent at all under a disturbance with high frequency components over band $[j\eta_c, +\infty)$.

To illustrate the relationship between $\lambda_2(L)$ and network coherence, we plot the step response of the Icelandic Power Grid [17] with 35 generators in Fig.2. In the original network, the generators are roughly coherent because, geographically, the scale of the network is small. To show how algebraic connectivity affects the coherence, we scale up all line susceptances by 10, which effectively scales up the $\lambda_2(L)$ by 10. It is clear from Fig.2 that the generators become more coherent when the $\lambda_2(L)$ is scaled up.

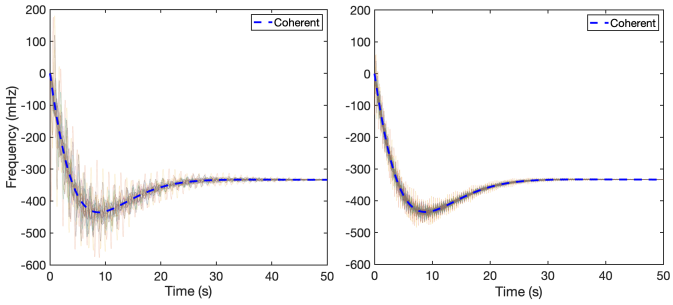

Fig. 2. Step response of Icelandic Grid without (Left) and with (Right) connectivity scaled up. The response of coherent dynamics $\hat{g}(s)$ is shown in blue dashed lines.

Interestingly, even when the network is not extremely coherent, the coherent dynamics $\hat{g}(s)$ seem to be a good network-independent representation of the global network response. We also refer to [14], where the synchronization cost, considered as a measure of coherence, is significantly reduced by adding lines (effectively increasing $\lambda_2(L)$) to the Icelandic Grid.

B. Aggregate Dynamics for Different Generator Models

Now we look into the explicit forms of the coherent dynamics $\hat{g}(s)$ for different generator models.

Example 1. *For generators given by the swing model*

$$g_i(s) = \frac{1}{m_i s + d_i},$$

where m_i, d_i are the inertia and damping of generator i, respectively. The aggregation dynamics are

$$\hat{g}(s) = \frac{1}{\hat{m}s + \hat{d}}, \tag{7}$$

where $\hat{m} = \sum_{i=1}^n m_i$ and $\hat{d} = \sum_{i=1}^n d_i$.

The aggregate model given by (7) is consistent with the conventional approach of choosing inertia $\hat{m}$ and damping $\hat{d}$ as the respective sums over all coherent generators. Theorem 1 explains why such a choice is indeed appropriate.

The aggregation is more complicated when considering generators with turbine droop control:

Example 2. *For generators given by the swing model with turbine droop*

$$g_i(s) = \frac{1}{m_i s + d_i + \frac{r_i^{-1}}{\tau_i s + 1}}, \tag{8}$$

where r_i^{-1} and τ_i are the droop coefficient and turbine time constant of generator i, respectively. The coherent dynamics are given by

$$\hat{g}(s) = \frac{1}{\hat{m}s + \hat{d} + \sum_{i=1}^n \frac{r_i^{-1}}{\tau_i s + 1}}. \tag{9}$$

This example illustrates, in particular, the difficulty in aggregating generators with heterogeneous turbine time constants. When all generators have the same turbine time constant $\tau_i = \hat{\tau}$, then $\hat{g}(s)$ in (9) reduces to the typical effective machine model

$$\hat{g}(s) = \frac{1}{\hat{m}s + \hat{d} + \frac{\hat{r}^{-1}}{\hat{\tau}s + 1}},$$

where $\hat{r}^{-1} = \sum_{i=1}^n r_i^{-1}$, i.e. the aggregation model is still obtained by choosing parameters $(\hat{m}, \hat{d}, \hat{r}^{-1})$ as the respective sums of their individual values.

However, if the τ_i are heterogeneous, then $\hat{g}(s)$ is a high-order transfer function and cannot be accurately represented by a single generator model. The aggregation of generators essentially asks for a low-order approximation of $\hat{g}(s)$.

III. Reduced Order Model for Coherent Synchronous Generators

As shown in the previous section, the coherent dynamics $\hat{g}(s)$ are of high-order if each generator has different turbine time constants. This suggests that substituting $\hat{g}(s)$ with an equivalent machine of the same order as each $g_i(s)$ may lead to substantial approximation error. In this section we propose instead a hierarchy of reduction models with increasing order, based on balanced realization theory [18], such that eventually an accurate reduction model is obtained as the order of the reduction increases. We further explore other avenues of improvement by applying the reduction methodology over the coherent dynamics itself, instead of the standard approach of applying a reduction only on the turbines [10], [11], [13].

A. Frequency Weighted Balanced Truncation

We first describe the methodology applied to derive the proposed reduced order models. Given a stable, strictly proper transfer function $G(s)$, a balanced realization is a state-space model (A, B, C), i.e. $\dot{x} = Ax + Bu$, $y = Cx$, such that its controllability and observability gramians (X_c and Y_o) are equal and diagonal ($X_c = Y_o = \mathrm{diag}(h_k)$, with $h_1 \geq \cdots \geq h_n \geq 0$). The $\{h_k\}$ are called Hankel singular values and measure the significance of each corresponding state. A *balanced truncation* $G_k(s)$ of order k, is obtained by keeping only the portions of (A, B, C) that involve the k-most significant states. Bounds can be given on the $\mathcal{H}_\infty$ norm of the approximation error $G(s) - G_k(s)$ as a function of the truncated h_k's, see [18]. In many cases, the Hankel singular values decay fast, which leads to $G_k(s)$ being an accurate approximation of $G(s)$.

One drawback of balanced truncation is that there is a non-negligible DC gain mismatch between the original and the reduced models, i.e. $G(0) \neq G_k(0)$, when k is not sufficiently large. To resolve this, we apply the balanced truncation with a stable LTI frequency weight $W(s)$. Compared to the unweighted method, the frequency weighted balanced truncation [19] favors accuracy in the frequency range where $W(s)$ is high. For our purpose, by choosing weights $W(s)$ which are large in the low frequency ranges, we effectively reduce the DC gain mismatch of our reduced order models. The detailed procedures of frequency weighted balanced truncation are described in appendix.

For the purpose of this paper, these details are not critical. It suffices to regard frequency weighted balanced truncation method as a tool that, given a single input single output proper transfer function $G(s)$, a frequency weight $W(s)$, and a number k, returns a transfer function

$$\tilde{G}_k(s) = \frac{b_{k-1}s^{k-1} + \cdots + b_1 s + b_0}{a_k s^k + \cdots + a_1 s + a_0}, \tag{10}$$

guaranteed to be stable [19], and such that the weighted error $\sup_{\eta\in\mathbb{R}} |W(j\eta)(G(j\eta) - \tilde{G}_k(j\eta))|$ is upper bounded, with an upper bound decreasing to zero with the order k. In the remaining of this section, we propose two model reduction approaches for high-order $\hat{g}(s)$ in (9) based on frequency weighted balanced truncation.

B. Model Reduction on Turbine Dynamics

Our first model is based on applying balanced truncation to the turbine aggregate. Essentially, $\hat{g}(s)$ in (9) is of high order because it has high-order turbine dynamics $\sum_{i=1}^n \frac{r_i^{-1}}{\tau_i s+1}$; we seek to replace it with a reduced order model. This is akin to the existing literature [10], [11] which replaces an aggregate of turbines in parallel by a first order turbine model with optimal parameters obtained by minimizing certain error functions.

We denote the aggregated turbine dynamics as

$$\hat{g}_t(s) := \sum_{i=1}^n \frac{r_i^{-1}}{\tau_i s + 1}.$$

We also denote the $(k-1)$-th reduction model of $\hat{g}_t(s)$ by frequency-weighted balanced truncation as $\tilde{g}_{t,k-1}(s)$. Then the k-th order reduction model of $\hat{g}(s)$ is given by

$$\tilde{g}_k^{tb}(s) = \frac{1}{\hat{m}s + \hat{d} + \tilde{g}_{t,k-1}(s)}, \tag{11}$$

with, again, $\hat{m} = \sum_{i=1}^n m_i$ and $\hat{d} = \sum_{i=1}^n d_i$.

We highlight two special instances of relevance for our numerical illustration.

1) 2nd order reduction model: When $k = 2$, the aggregate turbine dynamics $\hat{g}_t(s)$ are approximated by a first order transfer function $\tilde{g}_{t,1}(s)$ which can be interpreted as a first order turbine model

$$\tilde{g}_{t,1}(s) = \frac{b_0}{a_1 s + a_0} = \frac{\tilde{r}^{-1}}{\tilde{\tau}s + 1},$$

with parameters $(\tilde{r}^{-1}, \tilde{\tau})$ chosen by the weighted balanced truncation method. Then the overall reduction model $\tilde{g}_2^{tb}(s)$ is second order, which is a single generator model.

Unlike [10], [11], there is a DC gain mismatch between $\tilde{g}_2^{tb}(s)$ and original $\hat{g}(s)$ since $\tilde{r}^{-1} \neq \hat{r}^{-1} = \sum_{i=1}^n r_i^{-1}$. Later in the simulation section, we will see that by choosing a proper frequency weight $W(s)$, we effectively make the DC gain mismatch negligible. Unfortunately, as we will see in the numerical section, $k = 2$ may not suffice to accurately approximate the coherent dynamics.

2) 3rd order reduction model: To obtain a more accurate reduced order model, one may consider $k = 3$ as the next suitable option. In fact, according to numerical observations, a 2nd order turbine model $\tilde{g}_{t,2}(s)$, i.e., $k = 3$, is sufficient to give an almost exact approximation of $\hat{g}_t(s)$. In this case, we have an overall 3rd order reduced model $\tilde{g}_3^{tb}(s)$.

We can also interpret $\tilde{g}_{t,2}(s)$, by means of partial fraction expansion, i.e.,

$$\tilde{g}_{t,2}(s) = \frac{b_1 s + b_0}{a_2 s^2 + a_1 s + a_0} = \frac{\tilde{r}_1^{-1}}{\tilde{\tau}_1 s + 1} + \frac{\tilde{r}_2^{-1}}{\tilde{\tau}_2 s + 1},$$

assuming the poles are real. Then the reduced turbine dynamics $\tilde{g}_{t,2}(s)$ can be interpreted as two first order turbines in parallel with parameters $(\tilde{r}_1^{-1}, \tilde{\tau}_1)$ and $(\tilde{r}_2^{-1}, \tilde{\tau}_2)$.

C. Model Reduction on Closed-loop Coherent Dynamics

Our second proposal is the following: instead of reducing the turbine dynamics (11), we apply weighted balanced truncation directly on $\hat{g}(s)$. Thus, we denote $\tilde{g}_k^{cl}(s)$ as the k-th order reduction model, via frequency weighted balanced truncation, of the coherent dynamics $\hat{g}(s)$. Again, although there may be a DC gain mismatch between $\tilde{g}_2^{cl}(s)$ and the original $\hat{g}(s)$, it can be made negligible by properly choosing $W(s)$.

As compared to Section III-B, the reduced model might not be easy to interpret in practice. Nevertheless, the procedure described below often leads to such an interpretation.

1) 2nd order reduction model: When $k = 2$, we wish to interpret $\tilde{g}_2^{cl}(s)$ in terms of a single generator with a first order turbine of the form in (8), with parameters $(\tilde{m}, \tilde{d}, \tilde{r}^{-1}, \tilde{\tau})$. Given

$$\tilde{g}_2^{cl}(s) = \frac{b_1 s + b_0}{a_2 s^2 + a_1 s + a_0} =: \frac{N(s)}{D(s)},$$

obtained via the proposed method: write the polynomial division $D(s) = Q(s)N(s) + R$, where $Q(s), R$ are quotient and remainder, respectively. Here the remainder R is a scalar because the divisor $N(s)$ is a first order polynomial of s. This leads to the expression

$$\tilde{g}_2^{cl}(s) = \frac{N(s)}{Q(s)N(s) + R} = \frac{1}{Q(s) + \frac{R}{N(s)}}.$$

Here the first order polynomial $Q(s)$ can be matched to $\tilde{m}s + \tilde{d}$, and $\frac{R}{N(s)}$ to $\frac{\tilde{r}^{-1}}{\tilde{\tau}s+1}$. Provided the obtained constants $(\tilde{m}, \tilde{d}, \tilde{r}^{-1}, \tilde{\tau})$ are positive, the interpretation follows.

2) 3rd order reduction model: Similarly, when $k = 3$, the reduced model is $\tilde{g}_3^{cl}(s) = \frac{N(s)}{D(s)}$, with $N(s)$ of 2nd order and $D(s)$ of 3rd order. The polynomial division $D(s) = Q(s)N(s) + R(s)$, still gives a first order quotient $Q(s)$, which is interpreted as $\tilde{m}s + \tilde{d}$; the second order transfer function $\frac{R(s)}{N(s)}$ can be expressed, by partial fraction expansion, as two first order turbines in parallel, provided the obtained constants remain positive. We explore this in the examples studied below.

IV. Numerical Simulations

We now evaluate the reduction methodologies proposed in the previous section, and compare their performance with the solutions proposed in [10], [11]. In our comparison, we consider 5 generators forming a coherent group. All parameters are expressed in a common base of 100 MVA.

The test case: 5 generators, $\hat{m} = 0.0683(\text{s}^2/\text{rad})$, $\hat{d} = 0.0107$. The turbine and droop parameters of each generator are listed in Table I. In all comparisons, a step change of -0.1 p.u. is used.

TABLE I
Droop control parameters of generators in test case

Parameter \ Index	1	2	3	4	5
droop r_i^{-1} (p.u.)	0.0218	0.0256	0.0236	0.0255	0.0192
time constant τ_i (s)	9.08	5.26	2.29	7.97	3.24

Remark. In the test case, we only aggregate 5 generators and report all parameters explicitly in order to give more insights on how the distribution of time constant τ_i affects our approximations. It is worth noting that similar behavior is observed when reducing coherent groups with a much larger number of generators. In particular, the accuracy found below with 3rd order reduced models is also observed in these higher order problems.

A. DC Gain Mismatch Cancellation

As mentioned in the previous section, one of the drawbacks of the balanced truncation method is that it does not match the DC gain of the original system, which leads to an error on the steady-state frequency. We illustrate this issue in Fig. 3, where we compare the step response of two 2nd order reduction models $\tilde{g}_2^{tb}(s)$ using frequency weighted balanced truncation on the turbines, with different weights: 1) unweighted: $W_1(s) = 1$; 2) weighted: $W_2(s) = \frac{s+3\cdot10^{-2}}{s+10^{-4}}$.

Fig. 3 compares step responses and Bode plots for the original coherent dynamics $\hat{g}(s)$ (solid gray) with those of reduced models (dotted and dashed lines).

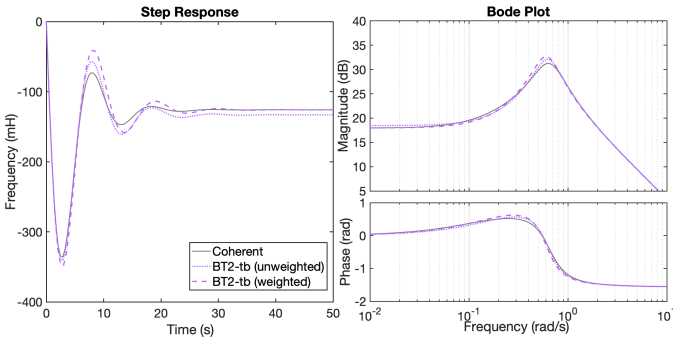

Fig. 3. Second order models by balanced truncation on turbine dynamics with frequency weights $W_1(s) = 1$ (unweighted) and $W_2(s) = \frac{s+3\cdot10^{-2}}{s+10^{-4}}$ (weighted). Step response (left) and Bode plot (right).

The DC gain mismatch is reflected in the steady state step response; we see that it is significantly reduced by frequency weighted balanced truncation. However, it gives worse approximation to $\hat{g}(s)$ in the transient phase than the unweighted truncation. The Bode plot also reflects such a trade-off: the unweighted model has lower approximation error around the peak gain ($0.1 - 1$ rad/s) of $\hat{g}(s)$, at the cost of inaccuracies in the low frequency range (< 0.1rad/s). The weighted model exhibits exactly the opposite behavior, as the weight $W_2(s) = \frac{s+3\cdot10^{-2}}{s+10^{-4}}$ puts more emphasis on low frequency ranges.

As we will show in Section IV-D, neither can optimization-based approaches get rid of this trade-off. This suggests that a second order model is not sufficient to fully recover our coherent dynamics $\hat{g}(s)$. The main reason is that the time constants τ_i have wide spread: from ~2s to ~9s. As the result, it is difficult to find a proper time constant $\tilde{\tau}$ to account for both fast and slow turbines. The way to resolve it is approximating $\hat{g}(s)$ by higher-order reduced models.

B. Effect of Reduction Order k in Accuracy

We now evaluate the effect of the order of the reduction in the accuracy. That is, we compare 2nd and 3rd order balanced truncation on, the turbine dynamics, i.e., $\tilde{g}_2^{tb}(s)$ (BT2-tb), $\tilde{g}_3^{tb}(s)$ (BT3-tb), as well as balanced truncation on the closed-loop coherent dynamics $\tilde{g}_2^{cl}(s)$ (BT2-cl), $\tilde{g}_3^{cl}(s)$ (BT3-cl). The frequency weights are given by $W_{tb}(s) = \frac{s+3\cdot 10^{-2}}{s+10^{-4}}$ and $W_{cl}(s) = \frac{s+8\cdot 10^{-2}}{s+10^{-4}}$, respectively. The step response along with step response error with respect to $\hat{g}(s)$ are shown in Fig. 4.

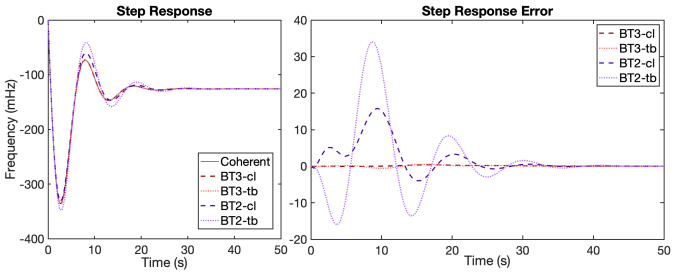

Fig. 4. Comparison of all reduced order models by balanced truncation

It is clear that, when compared with 2nd order models, 3rd order reduced models give a very accurate approximation of $\hat{g}(s)$. While it is not surprising that approximation models with higher order ($k = 3$) outperform models with lower order ($k = 2$), we highlight that with only a third order model one can accurately approximate the entire aggregate response.

Moreover, when we examine the transfer function given by $\tilde{g}_3^{tb}(s)$ (from input u in p.u. to output w in rad/s), we find an interesting interpretation. That is, the turbine model for $\tilde{g}_3^{tb}(s)$ is given by

$$\tilde{g}_{t,2}(s) = \frac{0.02664s + 0.00566}{s^2 + 0.5046s + 0.04891},$$

which, after doing partial fraction expansion, gives

$$\tilde{g}_{t,2}(s) = \frac{0.0473}{2.6759s + 1} + \frac{0.0684}{7.64s + 1}.$$

The latter can be viewed as two turbines (one fast turbine and one slow turbine) in parallel, and the choices of droop coefficients for these two turbines reflects the aggregate droop coefficients of fast turbines (generator 3,5) and slow turbines (generator 1,2,4), respectively, in $\hat{g}(s)$.

C. Reduction on Turbines vs. Closed-loop Coherent Dynamics

Another interesting observation that can also be derived from Fig. 4 is that balanced truncation on the closed-loop is more accurate than balanced truncation on the turbine. To get a more straightforward comparison, we list in Table II the approximation errors of all 4 models in Fig 4 using the following metrics: 1) $\mathcal{L}_2$-norm of step response error $e(t)$ (in rad/s): $(\int_0^{+\infty} |e(t)|^2 dt)^{1/2}$; [1] 2) $\mathcal{L}_\infty$-norm of $e(t)$: $\max_{t\geq 0} |e(t)|$; 3) $\mathcal{H}_\infty$-norm difference between reduced and original models (from input u in p.u. to output w in rad/s).

[1]For reduced order models obtained via frequency weighted balanced truncation, there exists extremely small but non-zero DC gain mismatch that makes the $\mathcal{L}_2$-norm unbounded. We resolve this issue by simply scaling our reduced order models to have exactly the same DC gain as $\hat{g}(s)$.

TABLE II
APPROXIMATION ERRORS OF REDUCED ORDER MODELS BY BALANCED TRUNCATION

Model \ Metric	$\mathcal{L}_2$ diff. (rad/s)	$\mathcal{L}_\infty$ diff. (rad/s)	$\mathcal{H}_\infty$ diff.
BT2-tb	4.3737	2.1454	7.5879
BT2-cl	2.0376	0.9934	2.0381
BT3-tb	0.0967	0.0361	0.1315
BT3-cl	0.0704	0.0249	0.0317

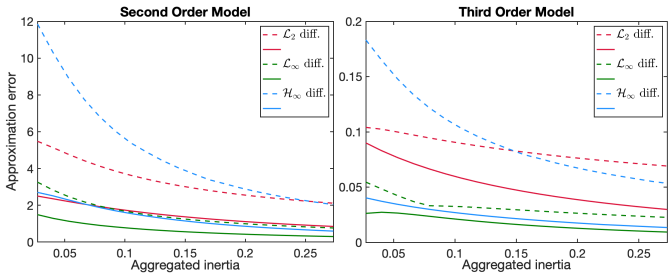

Fig. 5. Approximation errors of second order models (left) and third order models (right) by balanced truncation. Different metrics are shown in different colors. Approximation errors of reduced order models $\tilde{g}_2^{tb}(s)$, $\tilde{g}_3^{tb}(s)$ by reduction on turbine dynamics are shown in dashed lines; Approximation errors of reduced order models $\tilde{g}_2^{cl}(s)$, $\tilde{g}_3^{cl}(s)$ by reduction on closed-loop dynamics are shown in solid lines.

We observe from Table II that for a given the reduction order, balanced truncation on the closed-loop dynamics ($\tilde{g}_2^{cl}(s)$, $\tilde{g}_3^{cl}(s)$) has smaller approximation error than balanced truncation on turbine dynamics ($\tilde{g}_2^{tb}(s)$, $\tilde{g}_3^{tb}(s)$) *across all metrics*. Such observation seems to be true in general. For instance, Fig. 5 shows a similar trend by plotting the same configuration (metrics and models) of Table II for different values of of the aggregate inertia $\hat{m}$, while keeping all other parameters the same.

It can be seen from Fig. 5 that reduction on closed-loop dynamics improves the approximation in every metric, uniformly, for a wide range of aggregate inertia $\hat{m}$ values. The main reason is that, when applying reduction on closed-loop dynamics, the algorithm has the flexibility to choose the corresponding values of inertia and damping to be different from the aggregate ones in order to better approximate the response. More precisely, we have

$$\begin{aligned}\tilde{g}_2^{cl}(s) &= \frac{14.89s + 2.994}{s^2 + 0.4191s + 0.3787} \\ &= \frac{4.9733s + 1}{(0.06715s + 0.01464)(4.9733s + 1) + 0.1118},\end{aligned}$$

from which we can get the equivalent swing and turbine model as

$$\text{swing model: } \frac{1}{0.06715s + 0.01464}, \text{ turbine: } \frac{0.1118}{4.9733s + 1}.$$

The equivalent inertia and damping are $\tilde{m} = 0.06715$ and $\tilde{d} = 0.01464$, which are different from the aggregated values $\hat{m}, \hat{d}$. Therefore, when compared to reduction on turbine dynamics, reduction on closed-loop dynamics is essentially less constrained on the parameter space, thus achieving smaller approximation errors.

D. Comparison with Existing Methods

Lastly, we compare reduced order models via balanced truncation on the closed-loop dynamics, $\tilde{g}_2^{cl}(s)$, $\tilde{g}_3^{cl}(s)$, with the solutions proposed in [10], [11]. The step responses and the approximation errors are shown in Fig. 6 and Table. III.

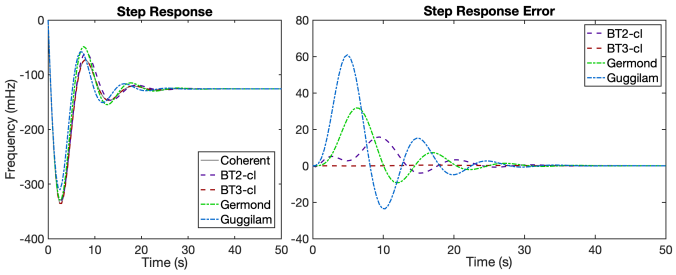

Fig. 6. Comparison of reduced order models

TABLE III
APPROXIMATION ERRORS OF REDUCED ORDER MODELS

Metric / Model	$\mathcal{L}_2$ diff. (rad/s)	$\mathcal{L}_\infty$ diff. (rad/s)	$\mathcal{H}_\infty$ diff.
Guggilam [11]	7.2956	3.8287	10.2748
Germond [10]	3.9594	1.9974	5.1431
BT2-cl	2.0376	0.9934	2.0381
BT3-cl	**0.0704**	**0.0249**	**0.0317**

In the comparison, $\tilde{g}_3^{cl}(s)$ outperforms all other reduced order models and it is the most **accurate reduced order model** of $\hat{g}(s)$. It is also worth noting that $\tilde{g}_2^{cl}(s)$ has the least approximation error among all 2nd order models. In general, such results suggest us that to improve the accuracy of reduced order model of coherent dynamics of generators $\hat{g}(s)$, we should consider: 1) increasing the complexity (order) of the reduction model; 2) reduction on closed-loop dynamics instead of on turbine dynamics.

V. CONCLUSION AND FUTURE WORK

This paper proposes a novel method to derive reduced order models for coherent generators. We derive a novel characterization of the aggregate response of coherent generators, i.e., $\hat{g}(s) = \left(\sum_{i=1}^n g_i^{-1}(s)\right)^{-1}$. We show that this aggregate dynamics $\hat{g}(s)$ is asymptotically accurate as the coupling between generators (characterized via $\lambda_2(L)$) increases. Our characterization not only explains why methods to aggregate generators with homogeneous time constants are accurate, but also explains the difficulties of aggregating generators with heterogeneous turbine time constants, i.e., when the coherent dynamics $\hat{g}(s)$ becomes a high-order transfer function. We solve this problem by leveraging tools from control theory to develop a methodology that finds accurate reduced order models of $\hat{g}(s)$. For $\{g_i(s)\}_{i=1}^n$ given by the 2nd order generator models, the numerical simulations show that 3rd order models based on frequency weighted balanced truncation on closed-loop dynamics is sufficient to accurately recover $\hat{g}(s)$.

There are many possible extensions to the existing results. Firstly, it has been shown in [14] that, whenever all the generator transfer functions $\{g_i(s)\}_{i=1}^n$ are proportional to each other, $\hat{g}(s)$ is a perfect descriptor of of the Center of Inertia (COI) frequency $\bar{w} = \left(\sum_{i=1}^n m_i w_i\right) / \left(\sum_{i=1}^n m_i\right)$. It is currently an on-going effort to show that $\hat{g}(s)$ is a reasonable approximation of the dynamics of COI frequency $\bar{w}$ even when the proportionality condition fails.

Further experimentation with higher-order generator models as well as an extension of our analysis to multiple groups of coherent generators is a subject of future research.

APPENDIX

A. Proof of the Theorem 1

To proof the theorem, we need to present two lemmas first:

Lemma 1. *Let A,B be matrices of order n. For **increasingly** ordered singular values $\sigma_i(A), \sigma_i(B)$, if $\sigma_1(A) \geq \sigma_n(B)$, then the following inequality holds:*

$$\|(A+B)^{-1}\| \leq \frac{1}{\sigma_1(A) - \sigma_n(B)} = \frac{1}{\sigma_1(A) - \|B\|}$$

Proof. By [20, 3.3.16], we have:

$$\sigma_1(A) \leq \sigma_1(A+B) + \sigma_n(-B)$$

Then as long as $\sigma_1(A) \geq \sigma_n(B)$, the following holds:

$$\frac{1}{\sigma_1(A+B)} \leq \frac{1}{\sigma_1(A) - \sigma_n(B)}$$

notice that the left-hand side is exactly $\|(A+B)^{-1}\|$. □

Lemma 2. *Let $\hat{g}(s), T(s)$ be defined in (4) and (5). Define $\bar{g}(s) := n\hat{g}(s)$. Suppose for $s_0 \in \mathbb{C}$, we have $|\bar{g}(s_0)| \leq M_1$ and $\max_{1\leq i\leq n} |g_i^{-1}(s_0)| \leq M_2$ for some $M_1, M_2 > 0$. Then for large enough $\lambda_2(L)$, the following inequality holds:*

$$\left\| T(s_0) - \frac{1}{n}\bar{g}(s_0)\mathbb{1}\mathbb{1}^T \right\| \leq \frac{M_1^2 M_2^2 + 2M_1 M_2 + \frac{M_1 M_2^2}{|\lambda_2(L)/s_0| - M_2}}{|\lambda_2(L)/s_0| - M_2 - M_1 M_2^2} + \frac{1}{|\lambda_2(L)/s_0| - M_2} \tag{12}$$

Proof. Since L is symmetric Laplacian matrix, the decomposition of L is given by:

$$L = V\Lambda V^T,$$

where $V = [\frac{\mathbb{1}_n}{\sqrt{n}}, V_\perp]$, $VV^T = V^TV = I_n$, and $\Lambda = \text{diag}\{\lambda_i(L)\}$ with $0 = \lambda_1(L) \leq \lambda_2(L) \leq \cdots \leq \lambda_n(L)$.

For the transfer matrix $T(s)$, we have:

$$\begin{aligned} T(s) &= (I_n + \text{diag}\{g_i(s)\}L/s)^{-1}\text{diag}\{g_i(s)\} \\ &= (\text{diag}\{g_i^{-1}(s)\} + L/s)^{-1} \\ &= (\text{diag}\{g_i^{-1}(s)\} + V(\Lambda/s)V^T)^{-1} \\ &= V(V^T\text{diag}\{g_i^{-1}(s)\}V + \Lambda/s)^{-1}V^T \end{aligned}$$

Let $H = V^T \text{diag}\{g_i^{-1}(s_0)\}V + \Lambda/s_0$, then it's easy to see that:

$$\begin{aligned}\left\|T(s_0) - \frac{1}{n}\bar{g}(s_0)\mathbb{1}_n\mathbb{1}_n^T\right\| &= \|T(s_0) - \bar{g}(s_0)Ve_1e_1^TV^T\| \\ &= \left\|V\left(H^{-1} - \bar{g}(s_0)e_1e_1^T\right)V^T\right\| \\ &= \left\|H^{-1} - \bar{g}(s_0)e_1e_1^T\right\| \qquad (13)\end{aligned}$$

We write H in block matrix form:

$$\begin{aligned}H =& \ V^T\text{diag}\{g_i^{-1}(s_0)\}V + \Lambda/s_0 \\ =& \begin{bmatrix}\frac{\mathbb{1}_n^T}{\sqrt{n}} \\ V_\perp^T\end{bmatrix}\text{diag}\{g_i^{-1}(s_0)\}\begin{bmatrix}\frac{\mathbb{1}_n}{\sqrt{n}} & V_\perp\end{bmatrix} + \Lambda/s_0 \\ =& \begin{bmatrix}\bar{g}^{-1}(s_0) & \frac{\mathbb{1}_n^T}{\sqrt{n}}\text{diag}\{g_i^{-1}(s_0)\}V_\perp \\ V_\perp^T\text{diag}\{g_i^{-1}(s_0)\}\frac{\mathbb{1}_n}{\sqrt{n}} & V_\perp^T\text{diag}\{g_i^{-1}(s_0)\}V_\perp + \tilde{\Lambda}/s_0\end{bmatrix} \\ :=& \begin{bmatrix}\bar{g}^{-1}(s_0) & h_{12}^T \\ h_{12} & H_{22}\end{bmatrix}\end{aligned}$$

where $\tilde{\Lambda} = \text{diag}\{\lambda_2(L), \cdots, \lambda_n(L)\}$.

Invert H in its block form, we have:

$$H^{-1} = \begin{bmatrix}a & -ah_{12}^TH_{22}^{-1} \\ -aH_{22}^{-1}h_{12} & H_{22}^{-1} + aH_{22}^{-1}h_{12}h_{12}^TH_{22}^{-1}\end{bmatrix}$$

where $a = \frac{1}{\bar{g}^{-1}(s_0) - h_{12}^TH_{22}^{-1}h_{12}}$.

Notice that:

$$\|h_{12}\| \le \frac{\|\mathbb{1}_n\|}{\sqrt{n}}\|\text{diag}\{g_i^{-1}(s_0)\}\|\|V_\perp\| \le M_2 \qquad (14)$$

Also, by Lemma 1, when $|\lambda_2(L)/s_0| > M_2$, the following holds:

$$\begin{aligned}\|H_{22}^{-1}\| \le& \ \frac{1}{\sigma_1(\tilde{\Lambda}) - \|V_\perp^T\text{diag}\{g_i^{-1}(s_0)\}V_\perp\|} \\ \le& \ \frac{1}{|\lambda_2(L)/s_0| - M_2} \qquad (15)\end{aligned}$$

Lastly, when $|\lambda_2(L)/s_0| > M_2 + M_2^2M_1$, by (14)(15), we have:

$$\begin{aligned}|a| \le& \ \frac{1}{|\bar{g}^{-1}(s_0)| - \|h_{12}\|^2\|H_{22}^{-1}\|} \\ \le& \ \frac{(|\lambda_2(L)/s_0| - M_2)M_1}{|\lambda_2(L)/s_0| - M_2 - M_1M_2^2} \qquad (16)\end{aligned}$$

Now we bound the norm of $H^{-1} - \bar{g}(s_0)e_1e_1^T$ by the sum of norms of all its blocks:

$$\begin{aligned}&\|H^{-1} - \bar{g}(s_0)e_1e_1^T\| \\ =& \left\|\begin{bmatrix}a\bar{g}(s_0)h_{12}^TH_{22}^{-1}h_{12} & -ah_{12}^TH_{22}^{-1} \\ -aH_{22}^{-1}h_{12} & H_{22}^{-1} + aH_{22}^{-1}h_{12}h_{12}^TH_{22}^{-1}\end{bmatrix}\right\| \\ \le& |a|\|H_{22}^{-1}\|(|\bar{g}(s_0)|\|h_{12}\|^2 + 2\|h_{12}\| + \|h_{12}\|^2\|H_{22}^{-1}\|) \\ &+ \|H_{22}^{-1}\| \qquad (17)\end{aligned}$$

by (14)(15)(16), we have the following:

$$\begin{aligned}&\|H^{-1} - \bar{g}(s_0)e_1e_1^T\| \\ \le& \frac{M_1^2M_2^2 + 2M_1M_2 + \frac{M_1M_2^2}{|\lambda_2(L)/s_0| - M_2}}{|\lambda_2(L)/s_0| - M_2 - M_1M_2^2} + \frac{1}{|\lambda_2(L)/s_0| - M_2} \qquad (18)\end{aligned}$$

this bound holds as long as $|\lambda_2(L)/s_0| > M_2 + M_2^2M_1$, and combining (13)(18) gives the desired inequality. □

Now we can proof theorem 1:

Proof. $\bar{g}(s)$ is stable because $\hat{g}(s)$ is stable, then $\bar{g}(s)$ is continuous on compact set $[-j\eta_0, j\eta_0]$. Then by [21, Theorem 4.15] there exists $M_1 > 0$, such that $\forall s \in [-j\eta_0, j\eta_0]$, we have $|\bar{g}(s)| \le M_1$. Similarly, because all $g_i(s)$ are minimum-phase, all $g_i^{-1}(s)$ are stable hence continuous on $[-j\eta_0, j\eta_0]$. Again there exists $M_2 > 0$, such that $\forall s \in [-j\eta_0, j\eta_0]$, we have $\max_{1\le i\le n}|g_i^{-1}(s)| \le M_2$.

Now we know that $\forall s \in [-j\eta_0, j\eta_0]$, we have $|\bar{g}(s)| \le M_1, \max_{1\le i\le n}|g_i^{-1}(s)| \le M_2$, i.e. the condition for Lemma 2 is satisfied for a common choice of $M_1, M_2 > 0$.

By Lemma 2, $\forall s \in [-j\eta_0, j\eta_0]$, we have:

$$\begin{aligned}&\left\|T(s) - \hat{g}(s)\mathbb{1}\mathbb{1}^T\right\| \\ \le& \frac{M_1^2M_2^2 + 2M_1M_2 + \frac{M_1M_2^2}{|\lambda_2(L)/s| - M_2}}{|\lambda_2(L)/s| - M_2 - M_1M_2^2} + \frac{1}{|\lambda_2(L)/s| - M_2}.\end{aligned}$$

Taking $\sup_{s\in[-j\eta_0, j\eta_0]}$ on both sides gives:

$$\begin{aligned}&\sup_{s\in[-j\eta_0, j\eta_0]}\left\|T(s) - \hat{g}(s)\mathbb{1}\mathbb{1}^T\right\| \\ \le& \frac{M_1^2M_2^2 + 2M_1M_2 + \frac{M_1M_2^2}{|\lambda_2(L)|/\eta_0 - M_2}}{|\lambda_2(L)|/\eta_0 - M_2 - M_1M_2^2} + \frac{1}{|\lambda_2(L)|/\eta_0 - M_2}.\end{aligned}$$

Lastly, take $\lambda_2(L) \to +\infty$ on both sides, the right-hand side gives 0 in the limit, which finishes the proof. □

B. Frequency Weighted balanced Truncation

Given a minimum realization of frequency weight $W(s)$ to be (A_W, B_W, C_W, D_W), the procedures of frequency weighted balanced truncation for a minimum, strictly proper and stable linear system (A, B, C) with order n are given as follow:

1) The extended system[2] is given by:

$$\left[\begin{array}{cc|c}A & \mathbb{0} & B \\ B_WC & A_W & \mathbb{0} \\ \hline D_WC & C_W & \mathbb{0}\end{array}\right] := \left[\begin{array}{c|c}\bar{A} & \bar{B} \\ \hline \bar{C} & \mathbb{0}\end{array}\right].$$

2) Compute the frequency weighted controllability and observability gramians X_c, Y_o from the gramians $\bar{X}_c, \bar{Y}_o$ of extended system:

$$\bar{X}_c = \int_0^\infty e^{\bar{A}t}\bar{B}\bar{B}^Te^{\bar{A}^Tt}dt, \ \bar{Y}_o = \int_0^\infty e^{\bar{A}^Tt}\bar{C}^T\bar{C}e^{\bar{A}t}dt$$

$$X_c = \begin{bmatrix}I_n & \mathbb{0}\end{bmatrix}\bar{X}_c\begin{bmatrix}I_n \\ \mathbb{0}\end{bmatrix}, \ Y_c = \begin{bmatrix}I_n & \mathbb{0}\end{bmatrix}\bar{Y}_c\begin{bmatrix}I_n \\ \mathbb{0}\end{bmatrix}$$

3) Perform the singular value decomposition of $X_c^{\frac{1}{2}}Y_oX_c^{\frac{1}{2}}$:

$$X_c^{\frac{1}{2}}Y_oX_c^{\frac{1}{2}} = U\Sigma U^*$$

[2]When $W(s) = 1$, the extended system is exactly the same as original (A, B, C), then the procedures give unweighted standard balanced truncation.

where U is unitary and Σ is diagonal, positive definite with its diagonal terms in decreasing order. Then compute the change of coordinates T given by:

$$T^{-1} = X_c^{\frac{1}{2}} U \Sigma^{-1}$$

4) Apply change of coordinates T on (A, B, C) to get its balanced realization (TAT^{-1}, TB, CT^{-1}). Then the k-th order $(1 \leq k \leq n)$ reduction model (A_k, B_k, C_k) is given by truncating (TAT^{-1}, TB, CT^{-1}) as the following:

$$A_k = \begin{bmatrix} I_k & \mathbb{0} \end{bmatrix} TAT^{-1} \begin{bmatrix} I_k \\ \mathbb{0} \end{bmatrix}$$
$$B_k = \begin{bmatrix} I_k & \mathbb{0} \end{bmatrix} TB$$
$$C_k = CT^{-1} \begin{bmatrix} I_k \\ \mathbb{0} \end{bmatrix}$$

Remark. Balanced truncation only applies to systems in state space. For a transfer function, one should apply balanced truncation to its minimum realization, then obtain reduced order transfer function from the state-space reduction model.

REFERENCES

[1] J. H. Chow, *Power system coherency and model reduction*. Springer, 2013.

[2] R. Podmore, "Identification of coherent generators for dynamic equivalents," *IEEE Trans. Power App. Syst.*, no. 4, pp. 1344–1354, 1978.

[3] E. P. de Souza and A. L. da Silva, "An efficient methodology for coherency-based dynamic equivalents," in *IEE Proceedings C (Generation, Transmission and Distribution)*, vol. 139, no. 5. IET, 1992, pp. 371–382.

[4] T. Hiyama, "Identification of coherent generators using frequency response," in *IEE Proceedings C (Generation, Transmission and Distribution)*, vol. 128, no. 5. IET, 1981, pp. 262–268.

[5] J. H. Chow, G. Peponides, P. Kokotovic, B. Avramovic, and J. Winkelman, *Time-scale modeling of dynamic networks with applications to power systems*. Springer, 1982, vol. 46.

[6] J. R. Winkelman, J. H. Chow, B. C. Bowler, B. Avramovic, and P. V. Kokotovic, "An analysis of interarea dynamics of multi-machine systems," *IEEE Trans. Power App. Syst.*, vol. PAS-100, no. 2, pp. 754–763, Feb 1981.

[7] R. Nath, S. S. Lamba, and K. s. P. Rao, "Coherency based system decomposition into study and external areas using weak coupling," *IEEE Trans. Power App. Syst.*, vol. PAS-104, no. 6, pp. 1443–1449, June 1985.

[8] R. Podmore, *Coherency in Power Systems*. New York, NY: Springer New York, 2013, pp. 15–38.

[9] P. M. Anderson and M. Mirheydar, "A low-order system frequency response model," *IEEE Trans. Power Syst.*, vol. 5, no. 3, pp. 720–729, 1990.

[10] A. J. Germond and R. Podmore, "Dynamic aggregation of generating unit models," *IEEE Trans. Power App. Syst.*, vol. PAS-97, no. 4, pp. 1060–1069, July 1978.

[11] S. S. Guggilam, C. Zhao, E. DallAnese, Y. C. Chen, and S. V. Dhople, "Optimizing DER participation in inertial and primary-frequency response," *IEEE Trans. Power Syst.*, vol. 33, no. 5, pp. 5194–5205, Sep. 2018.

[12] D. Apostolopoulou, P. W. Sauer, and A. D. Domínguez-García, "Balancing authority area model and its application to the design of adaptive AGC systems," *IEEE Trans. Power Syst.*, vol. 31, no. 5, pp. 3756–3764, Sep. 2016.

[13] M. L. Ourari, L.-A. Dessaint, and V.-Q. Do, "Dynamic equivalent modeling of large power systems using structure preservation technique," *IEEE Trans. Power Syst.*, vol. 21, no. 3, pp. 1284–1295, 2006.

[14] F. Paganini and E. Mallada, "Global analysis of synchronization performance for power systems: bridging the theory-practice gap," *IEEE Trans. Automat. Contr.*, pp. 1–16, 2019, Early Access.

[15] H. Min and E. Mallada, "Dynamics concentration of large-scale tightly-connected networks," *arXiv preprint arXiv:1903.06017*, 2019.

[16] M. Fiedler, "Algebraic connectivity of graphs," *Czechoslovak Mathematical Journal*, vol. 23, no. 2, pp. 298–305, 1973.

[17] U. of Edinburgh. Power systems test case archive. [Online]. Available: https://www.maths.ed.ac.uk/optenergy/NetworkData/icelandDyn/

[18] K. Zhou, J. C. Doyle, and K. Glover, *Robust and Optimal Control*. Upper Saddle River, NJ, USA: Prentice-Hall, Inc., 1996.

[19] S. W. Kim, B. D. Anderson, and A. G. Madievski, "Error bound for transfer function order reduction using freqeuncy weighted balanced truncation," *Systems & Control Letters*, vol. 24, no. 3, pp. 183 – 192, 1995.

[20] R. A. Horn and C. R. Johnson, *Matrix Analysis*, 2nd ed. New York, NY, USA: Cambridge University Press, 2012.

[21] W. Rudin *et al.*, *Principles of mathematical analysis*. McGraw-hill New York, 1964, vol. 3.